Ascorbate Deficiency Does Not Limit Nonphotochemical Quenching in *Chlamydomonas reinhardtii*[1][OPEN]

André Vidal-Meireles,[a] Dávid Tóth,[a,b] László Kovács,[a] Juliane Neupert,[c] and Szilvia Z. Tóth[a,2,3]

[a]Institute of Plant Biology, Biological Research Centre, Szeged, Hungary
[b]Doctoral School of Biology, University of Szeged, Szeged, Hungary
[c]Max-Planck Institut für Molekulare Pflanzenphysiologie, Potsdam-Golm, Germany

ORCID ID: 0000-0003-3419-829X (S.Z.T.).

Ascorbate (Asc; vitamin C) plays essential roles in development, signaling, hormone biosynthesis, regulation of gene expression, stress resistance, and photoprotection. In vascular plants, violaxanthin de-epoxidase requires Asc as a reductant; thereby, Asc is required for the energy-dependent component of nonphotochemical quenching (NPQ). To assess the role of Asc in NPQ in green algae, which are known to contain low amounts of Asc, we searched for an insertional *Chlamydomonas reinhardtii* mutant affected in the*VTC2* gene encoding GDP-L-Gal phosphorylase, which catalyzes the first committed step in the biosynthesis of Asc. The *Crvtc2-1* knockout mutant was viable and, depending on the growth conditions, contained 10% to 20% Asc relative to its wild type. When *C. reinhardtii* was grown photomixotrophically at moderate light, the zeaxanthin-dependent component of NPQ emerged upon strong red illumination both in the *Crvtc2-1* mutant and in its wild type. Deepoxidation was unaffected by Asc deficiency, demonstrating that the Chlorophycean violaxanthin de-epoxidase found in *C. reinhardtii* does not require Asc as a reductant. The rapidly induced, energy-dependent NPQ component characteristic of photoautotrophic *C. reinhardtii* cultures grown at high light was not limited by Asc deficiency either. On the other hand, a reactive oxygen species-induced photoinhibitory NPQ component was greatly enhanced upon Asc deficiency, both under photomixotrophic and photoautotrophic conditions. These results demonstrate that Asc has distinct roles in NPQ formation in *C. reinhardtii* as compared to vascular plants.

Ascorbate (Asc) is a multifunctional metabolite essential for a range of cellular processes in green plants, including cell division, stomatal movement, biosynthesis of various plant hormones, epigenetic regulation, and reactive oxygen species (ROS) scavenging (Asada, 2006; Foyer and Shigeoka, 2011; Smirnoff, 2018). Within the chloroplast, Asc may also act as an alternative electron donor to PSII and PSI (Ivanov et al., 2007; Tóth et al., 2009; Tóth et al., 2011). In vascular plants, violaxanthin de-epoxidase (VDE) requires Asc as a reductant, whereby Asc plays an essential role in the process of nonphotochemical quenching (NPQ) to dissipate excess energy as heat (Bratt et al., 1995; Saga et al., 2010; Hallin et al., 2016).

To fulfill the multiple physiological roles of Asc (reviewed by Smirnoff, 2018; Tóth et al., 2018), vascular plants maintain their Asc concentration at a high, ~20–30 mM level (Zechmann et al., 2011), which is also relatively constant, usually with no more than 2-fold increases upon stress treatments and moderate decreases during dark periods (Dowdle et al., 2007). Notwithstanding, Asc concentration may be limiting under environmental stress conditions, as shown by increased oxidative stress tolerance of plants overexpressing dehydroascorbate reductase, which is essential in Asc regeneration (Wang et al., 2010). Asc-deficient Arabidopsis (*Arabidopsis thaliana*) plants have slowly inducible and diminished NPQ, whereas Asc-overproducing plants possess enhanced NPQ relative to wild-type plants, indicating that Asc may limit the conversion of violaxanthin to zeaxanthin in vivo (Müller-Moulé et al., 2002; Tóth et al., 2011). Asc-deficient plants are also sensitive to high light, especially in combination with zeaxanthin deficiency (Müller-Moulé et al., 2003).

[1]This work was supported by the Lendület/Momentum Programme of the Hungarian Academy of Sciences (LP-2014/19), the National, Research and Development Office (NN 114524 and GINOP-2.3.2-15-2016-00026), and the Alexander von Humboldt Foundation (grants to S.Z.T.). A.V.-M. received fellowships from the Society for Experimental Biology/Company of Biologists Travel Fund, the U.S. Department of Energy Travel Award, and the International Society of Photosynthesis Research (sponsored by Wiley on behalf of Plant, Cell, and Environment).

[2]Senior author.
[3]Author for contact: toth.szilviazita@brc.hu.
The author responsible for distribution of materials integral to the findings presented in this article in accordance with the policy described in the Instructions for Authors (www.plantphysiol.org) is: Szilvia Z. Tóth (toth.szilviazita@brc.hu).

A.V.-M., J. N., and D.T. characterized the *Crvtc2-1* mutant and generated the complementation lines. L.K. developed the carotenoid content determination method. A.V.-M. performed the chl *a* fluorescence measurements, immunoblot analyses, and ascorbate content measurements. S.Z.T. conceived the study, analyzed the data, and wrote the article. A.V.-M., L.K., and J.N. contributed to analyzing the data and writing the article.
[OPEN]Articles can be viewed without a subscription.
www.plantphysiol.org/cgi/doi/10.1104/pp.19.00916

Green algae, such as *Chlamydomonas reinhardtii*, produce Asc in small amounts under favorable environmental conditions (~100–400 μM; Gest et al., 2013) and boost Asc levels only when needed, for instance upon a sudden increase in light intensity or nutrient deprivation (Vidal-Meireles et al., 2017; Nagy et al., 2018). Regulation of Asc biosynthesis differs significantly between plants and *C. reinhardtii*: in contrast to vascular plants, (1) green algal Asc biosynthesis is directly regulated by ROS; (2) it is not under circadian clock control; and (3) instead of a negative feedback regulation, there is a feedforward mechanism on the expression of the key Asc biosynthesis gene, *VTC2* (*Cre13.g588150*, encoding GDP-L-Gal phosphorylase), by Asc in the physiological concentration range (Vidal-Meireles et al., 2017).

VDE found in Chlorophyceae (CVDE) is not homologous to plant VDE but is related to a lycopene cyclase of photosynthetic bacteria (Li et al., 2016a). *C. reinhardtii* CVDE (CrCVDE), encoded by *Cre04.g221550*, has a FAD-binding domain and is located on the stromal side and not in the thylakoid lumen, as is the case for plant-type VDE (Li et al., 2016a). The cofactor or reductant requirement of the CrCVDE enzyme has not been investigated, and it is not known whether its activity requires Asc, either directly or indirectly.

Due to the major differences in Asc content, regulation of Asc biosynthesis, and VDE enzymes of vascular plants and Chlorophyceae, we decided to assess the role of Asc in the various NPQ components in *C. reinhardtii*. To this end, we characterized an insertional *VTC2* mutant procured from the Chlamydomonas Library Project (CLiP; Li et al., 2016b), which possesses only 10% to 20% of Asc relative to its parent strain. We have found that, in contrast to how it affects vascular plants, Asc deficiency does not limit energy-dependent quenching (qE) and violaxanthin de-epoxidation in *C. reinhardtii*; instead, Asc deficiency leads to enhanced photoinhibitory quenching (qI) upon excessive illumination.

RESULTS

Identification and Initial Characterization of an Asc-Deficient *VTC2* Insertional Mutant of *C. reinhardtii* and Its Genetic Complementation

To investigate the function of Asc in NPQ in *C. reinhardtii*, we searched for insertion mutants of *VTC2* in the CLiP library (Li et al., 2016b). We found one putative *VTC2* mutant (strain LMJ.RY0402.058624, hereafter *Crvtc2-1* mutant) holding one insertion of the paromomycin resistance (CIB1) casette at the junction site of exon 3 and the adjacent upstream intron of *VTC2* (Fig. 1A). The other available mutants were affected in the 3′ untranslated region (UTR) of *VTC2* and/or had multiple insertions in genes other than *VTC2* and thus were found unsuitable for this study. Due to the lack of another, independent CIB insertional mutant line affecting only *VTC2*, we carried out several NPQ measurements on our previously published *VTC2*-artificial microRNA (amiRNA) line (Vidal-Meireles et al., 2017) to confirm our findings on the consequences of Asc deficiency for NPQ (see below).

The site of CIB1 casette integration in the CLiP mutants had been validated by the LEAP-Seq method (Li et al., 2016b), and we verified the insertion site in the *Crvtc2-1* mutant by PCR (Fig. 1B). Using primers annealing upstream of the predicted insertion site in *VTC2*, a specific 852-bp fragment was observed in genomic DNA samples isolated from wild-type *C. reinhardtii* cells (CC-4533) and from the *Crvtc2-1* mutant strain (Fig. 1B, top); using primers designed to amplify the 5′ and 3′ junction sites of the CIB1 cassette, specific 470- and 601-bp fragments could be detected in the *Crvtc2-1* mutant (Fig. 1B, middle and bottom). Sequencing analysis of the PCR amplicons confirmed the predicted insertion of the CIB1 cassette in antisense orientation with its 5′ junction in exon 3 of the gene and the 3′ junction reaching to the adjacent intron upstream of exon 3 (Supplemental Fig. S1).

Under moderate light (100 μmol photons m^{-2} s^{-1}) and photomixotrophic conditions (growth in Tris-acetate-phosphate [TAP] medium), the wild-type strain (CC-4533) had ~12 pmol Asc/μg chlorophyll (Chl) $a+b$ (Fig. 1C), corresponding to ~200 μM cellular Asc concentration (see Kovács et al., 2016 for calculations), and the *Crvtc2-1* mutant had an Asc content only ~10% of the wild-type content. When the cultures were treated with 1.5 mM hydrogen peroxide (H_2O_2), which results in a strong increase in Asc content (Urzica et al., 2012; Vidal-Meireles et al., 2017), the Asc content increased ~3-fold in the wild type, whereas it did not increase in the *Crvtc2-1* mutant (Fig. 1C). This is in contrast to the *VTC2*-amiRNA lines generated earlier, where H_2O_2 treatment resulted in noticeable Asc accumulation (Vidal-Meireles et al., 2017).

Reverse transcription quantitative PCR (RT-qPCR) analysis with primers located upstream and downstream of the insertion site of the CIB1 cassette did not detect *VTC2* transcripts in the *Crvtc2-1* mutant samples grown under normal growth conditions or treated with H_2O_2 (Fig. 1D). Similarly, RT-PCR analysis using primers spanning the sequence encoding the catalytic site of *VTC2* (which is located downstream of the CIB1 casette insertion site) did not detect transcripts in the *Crvtc2-1* mutant under normal growth conditions, and only a weak signal was observed upon 35 PCR cycles in the H_2O_2-treated *Crvtc2-1* mutant samples (Fig. 1E).

To confirm that the decrease in Asc content was caused by the functional deletion of *VTC2* in the insertional mutant strain, we performed genetic complementation. To this end, we transformed the *Crvtc2-1* insertional mutant with the coding sequence of *VTC2* controlled by the constitutive promoter *PsaD*. Because the plasmid used for transformation included the *APH7″* resistance gene (Fig. 2A), its ability to grow on a medium containing hygromycin-B was used as the first screening method for successful transformation.

The integration of the plasmid in the genome was verified by PCR. Using a forward primer annealing to

the *PSAD* promoter region and a reverse primer annealing to the 5′ end of the *VTC2* coding sequence, a specific 841-bp fragment was amplified in genomic DNA samples isolated from two independent complementation lines of *Crvtc2-1+VTC2* (Fig. 2B). The *VTC2* transcript was detected in the complemented *Crvtc2-1+VTC2* lines via RT-PCR analysis with primers spanning the sequence encoding the catalytic site (Fig. 2C). The Asc content of the complementation lines was considerably restored (Fig. 2D). The cell volume, the cellular Chl content, and Chl *a/b* ratios were moderately increased in the *Crvtc2-1* mutant relative to the wild type, and these parameters were partially restored upon complementation (Supplemental Fig. S2, A–C).

No significant difference was observed in growth phenotypes between the strains when grown in TAP medium at 100 μmol photons m^{-2} s^{-1}, whereas the growth of the *Crvtc2-1* mutant was severely inhibited in TAP medium at 530 μmol photons m^{-2} s^{-1}, which was restored upon genetic complementation. In high salt (HS) medium at 530 μmol photons m^{-2} s^{-1}, growth was slow in all genotypes, and no significant differences were observed among them (Supplemental Fig. S2D). The Asc content increased 2- to 3-fold in each strain upon high light treatment, and the Asc content of

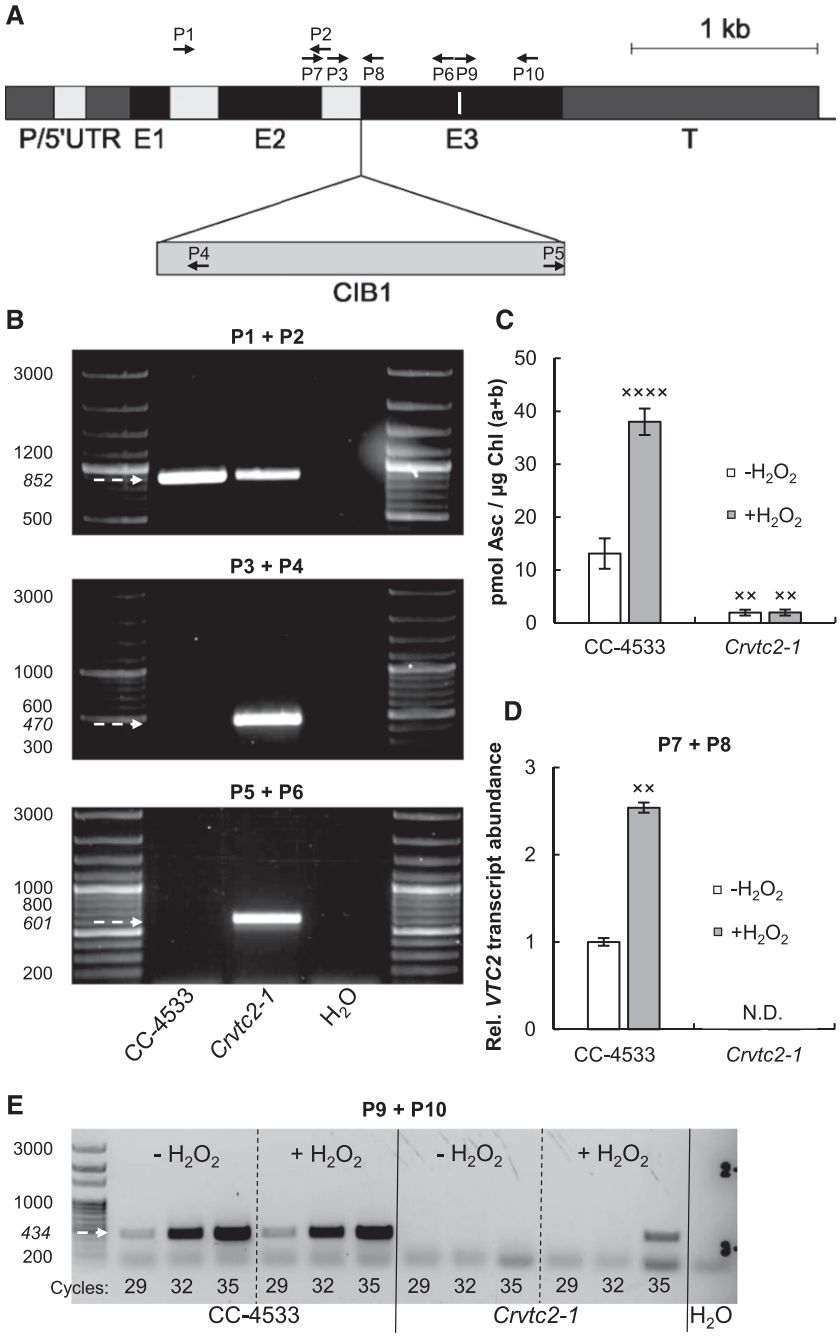

Figure 1. Characterization of an insertional CLiP mutant of *C. reinhardtii* (*Crvtc2-1*; LMJ.RY0402.058624) affected in the *VTC2* gene that encodes GDP-L-Gal phosphorylase. A, Physical map of *VTC2* (obtained from Phytozome, version 12.1.6) with the CIB1 cassette insertion site in the *Crvtc2-1* mutant. Exons are shown in black, introns in light gray, and promoter/5′ UTR and terminator sequences in dark gray. The insertion site of the CIB1 cassette is indicated by the triangle, and the binding sites of the primers used for genotyping and gene expression analysis of *Crvtc2-1* are shown as black arrows. The sequence encoding the catalytic site of GDP-L-Gal phosphorylase is marked as a white line within Exon 3. B, PCR performed using primers annealing upstream of the predicted cassette insertion site in *VTC2* (top, primers P1+P2) and primers amplifying the 5′ and 3′ genome-cassette junctions (middle and bottom; P3+P4 and P5+P6, respectively). The expected sizes are marked with arrows. C, Ascorbate contents of the wild type (CC-4533) and the *Crvtc2-1* mutant grown mixotrophically in TAP medium at moderate light with and without the addition of 1.5 mM H_2O_2. D, Transcript levels of *VTC2*, as determined by RT-qPCR in cultures supplemented, or not, with H_2O_2 using primers P7 and P8. E, Electrophoresis of RT-PCR products using primers P9 and P10, spanning the sequence that encodes the catalytic site of GDP-L-Gal phosphorylase. The number of PCR cycles is indicated at the bottom of the figure. The presented data are based on three independent experiments. When applicable, averages and SES (±SE) were calculated. Data were analyzed by one-way ANOVA followed by Dunnett's posttest: ×, $P < 0.05$, ××, $P < 0.01$, and ××××, $P < 0.0001$, compared to the untreated CC-4533 strain.

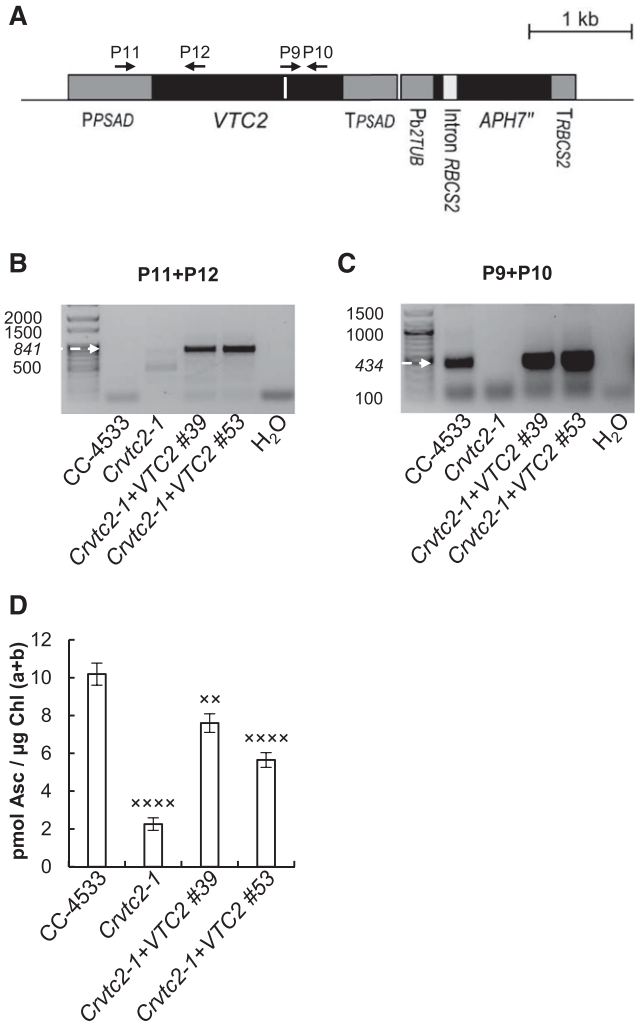

Figure 2. Complementation of the insertional CLiP mutant LMJ.RY0402.058624 (*Crvtc2-1*) affected in the *VTC2* gene with the coding sequence of *VTC2*. A, Physical map of the *Crvtc2-1+VTC2* plasmid containing the coding sequence of *VTC2*, the constitutive promoter *PsaD*, and the *APH7''* resistance gene and the terminators T*PSAD* and T*RBCS2*. Exons are shown in black and promoter/5′ UTR terminator sequences in dark gray, and the sequence encoding the catalytic site of GDP-L-Gal phosphorylase is marked as a white line. The binding sites of the primers used are shown as black arrows. B, PCR performed using primers annealing in the promoter and *VTC2* exon 1 (P11+P12). The expected size is marked with an arrow. C, Electrophoresis of RT-PCR products obtained using primers annealing to the sequence encoding the catalytic site of *VTC2* (P9+P10). The expected size is marked with an arrow. D, Ascorbate contents of CC-4533, the *Crvtc2-1* mutant, and the complementation lines *Crvtc2-1+VTC2* grown for 3 d in TAP at 100 μmol photons m^{-2} s^{-1}. The presented data are based on four independent experiments. When applicable, averages and SES (±SE) were calculated. Data were analyzed by one-way ANOVA followed by Dunnett's post-test: ××, $P < 0.05$ and ××××, $P < 0.0001$, compared to the CC-4533 strain. μE, μmol photons m^{-2} s^{-1}.

the *Crvtc2-1* mutant remained at a level of 10% to 20% relative to that of the wild type and the complementation lines (Supplemental Fig. S2E).

Effects of Asc Deficiency on NPQ in Cultures Grown at Normal Light and Photomixotrophic Conditions

NPQ includes short-term responses to changes in light intensity, as well as responses that occur over longer periods allowing for acclimation to high light exposure. In *C. reinhardtii*, the levels of the different NPQ components are variable and highly dependent on the growth conditions (Niyogi et al., 1997; Finazzi et al., 2006; Iwai et al., 2007; Peers et al., 2009).

In a first set of experiments to assess the effects of Asc deficiency on NPQ, *C. reinhardtii* strains were cultured in TAP medium at 100 μmol photons m^{-2} s^{-1}. Before the NPQ measurements, cultures were dark-adapted for about 30 min with shaking to avoid anaerobiosis; this dark adaptation protocol ensures the relaxation of most NPQ processes and the separation of the NPQ components induced under high light illumination (Roach and Na, 2017). When subjecting the cells to continuous red light of 530 μmol photons m^{-2} s^{-1}, a small, rapidly induced NPQ component was induced in the wild type and the Asc-deficient *Crvtc2-1* strain in the first 2 min (Fig. 3A) that we attribute to qE. qE is activated by low lumen pH, which occurs, for instance, during the induction of photosynthesis and upon CO_2 limitation of the Calvin-Benson-Bassham cycle (Kanazawa and Kramer, 2002; Takizawa et al., 2008). In *C. reinhardtii*, qE formation also requires zeaxanthin or lutein (Erickson et al., 2015) and is enhanced by a stress-related light harvesting complex (LHC) protein, LHCSR3, which is strongly expressed when algae are grown at high light (Peers et al., 2009; Bonente et al., 2011; Xue et al., 2015; Chaux et al., 2017). At moderate light (100 μmol photons m^{-2} s^{-1}) and photomixotrophic growth conditions, the LHCSR3 level was relatively low, particularly in the *Crvtc2-1* strain (Supplemental Fig. S3). The presence of acetate also enables high Calvin-Benson-Bassham cycle activity and a relatively low qE (Johnson and Alric, 2012), in agreement with our findings.

A slower NPQ component, induced on the timescale of several minutes, was also present, which was enhanced in the Asc-deficient *Crvtc2-1* mutant (Fig. 3A) and restored in its complementation strains (Supplemental Fig. S4A). This slow component was enhanced in our previously published *VTC2*-amiRNA line relative to its control strain as well (Supplemental Fig. S4C).

Three components may be responsible for this slowly induced NPQ component (see Allorent et al., 2013; Erickson et al., 2015): (1) zeaxanthin-dependent quenching (qZ), which may act on NPQ directly (e.g. Holt et al., 2005; Holub et al., 2007; Avenson et al., 2008), or indirectly by controlling the sensitivity of qE to the pH gradient or promoting conformational

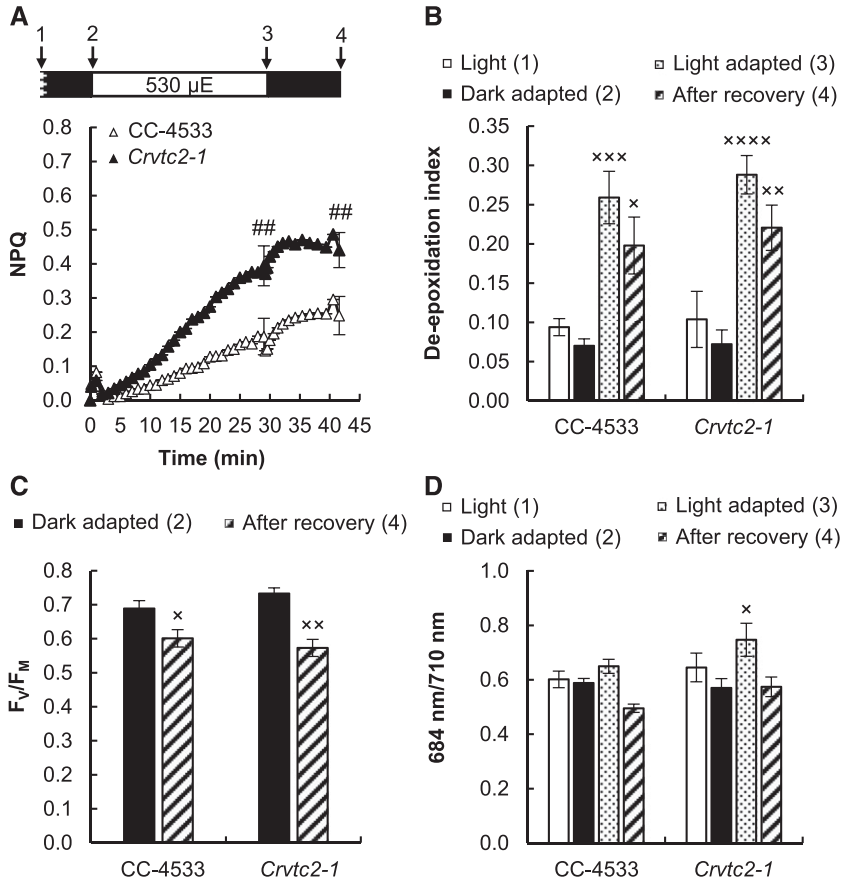

Figure 3. Acclimation to 530 μmol photons m^{-2} s^{-1} of red light followed by recovery in CC-4533 (wild type) and *Crvtc2-1* cultures grown photomixotrophically in TAP medium at 100 μmol photons m^{-2} s^{-1}. A, NPQ kinetics. Data were analyzed by one-way ANOVA followed by Dunnett's posttest: ##, $P < 0.01$, compared to the CC-4533 strain at the respective time point. μE, μmol photons m^{-2} s^{-1}. B, De-epoxidation index. C, The F_V/F_M value, an indicator of photosynthetic efficiency, parameter measured after dark adaptation and after recovery from the 530 μmol photons m^{-2} s^{-1} red light. D, The 684/710 nm ratio of the 77 K fluorescence spectra. Samples were collected at the growth light of 100 μmol photons m^{-2} s^{-1} after 30 min of dark adaptation, at the end of the 30-min light period with 530 μmol photons m^{-2} s^{-1}, and 15 min after the cessation of actinic illumination, as indicated by arrows in the scheme in A. The presented data are based on five independent experiments. When applicable, averages and SES (±SE) were calculated. Data were analyzed by one-way ANOVA followed by Dunnett's posttest: ×, $P < 0.05$, ××, $P < 0.01$, and ×××, $P < 0.001$, compared to the dark-adapted CC-4533 strain.

changes within LHCs (e.g. Johnson et al., 2008; Ruban et al., 2012); (2) state transition-dependent quenching (qT), which may contribute to balancing excitation energy between PSII and PSI via LHCII phosphorylation and antenna dissociation from PSII (Depège et al., 2003; Lemeille et al., 2009; Ünlü et al., 2014); and (3) a slowly relaxing qI associated with PSII damage or slowly reversible down-regulation of PSII representing a continuous form of photoprotection (Adams et al., 2013; Tikkanen et al., 2014).

To decipher the origin of the slow NPQ component and to study the possible role of Asc in NPQ, carotenoids were analyzed first using HPLC. Upon illumination, the de-epoxidation index largely increased (from ~0.05 to 0.25) both in the CC-4533 (wild type) strain and the *Crvtc2-1* mutant, and de-epoxidation only moderately recovered after the cessation of actinic illumination in both strains (Fig. 3B). Violaxanthin, antheraxanthin, and zeaxanthin concentrations were essentially the same in the *Crvtc2-1* mutant and in the wild type (Supplemental Fig. S5, A–C). These results suggest that qZ was partially responsible for the slow NPQ component and that Asc deficiency does not limit the de-epoxidation reaction. We also found that the amounts of β-carotene and lutein were not affected by the lack of Asc and their quantities remained constant during the entire protocol (Supplemental Fig. S5, D and E). The F_V/F_M values of dark-adapted cultures and those subjected to high light illumination followed by a recovery period were also very similar, with no major differences between the Asc-deficient mutant and the CC-4533 strain (Fig. 3C).

Since the de-epoxidation ratios were the same in the CC-4533 strain and in the *Crvtc2-1* mutant (Fig. 3B), it is likely that Asc deficiency does not limit the reaction. To completely exclude this possibility, a 16-h dark acclimation experiment was conducted, ensuring undetectably low levels of Asc (Fig. 4A). Still, NPQ was induced slowly upon illumination (Fig. 4B), and the de-epoxidation indices were similar to those in cultures subjected to relatively short dark adaptation (compare Figs. 3B and 4C); we note that during a 30-min illumination Asc does not accumulate (Vidal-Meireles et al., 2017).

The large increase in the de-epoxidation index upon illumination suggests that qZ is at least partially responsible for the slow NPQ component. However, we also observed that the slow NPQ component was larger in the *Crvtc2-1* mutant than in the wild type, whereas the de-epoxidation ratios were the same (Fig. 3, A and B). In addition to qZ, the qT and qI mechanisms may also contribute to the slow component, and they may differ between the wild type and the *Crvtc2-1* mutant. The possible contribution of

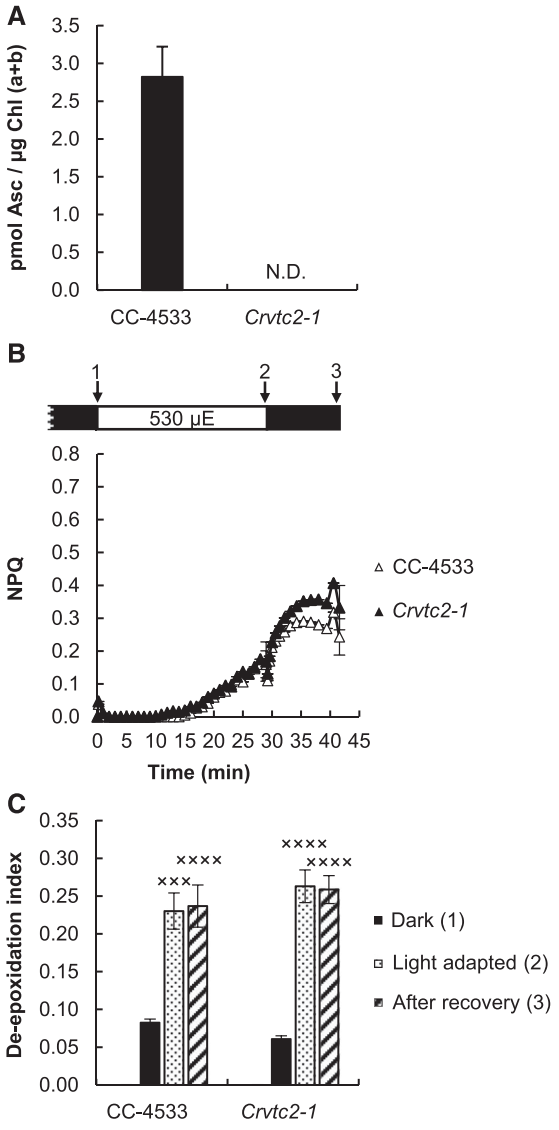

Figure 4. Effects of overnight (16 h) dark acclimation on CC-4533 and *Crvtc2-1* grown in TAP medium at 100 μmol photons m^{-2} s^{-1}. A, Ascorbate content after 16 h of dark acclimation. N.D., not detectable. B, NPQ, induced by 530 μmol photons m^{-2} s^{-1} of red light after overnight dark acclimation. μE, μmol photons m^{-2} s^{-1}. C, De-epoxidation index, determined in the overnight dark-acclimated cultures following red-light illumination and recovery. The presented data are based on four independent experiments. When applicable, averages and SES (±SE) were calculated. Data were analyzed by one-way ANOVA followed by Dunnett's posttest: ×××, $P < 0.001$, and ××××, $P < 0.0001$, compared to the dark-acclimated CC-4533 strain.

qT was studied by measuring 77 K fluorescence spectra: upon illumination with 530 μmol photons $m^{-2}s^{-1}$ red light, the 684/710 nm ratio remained unaltered in the wild type and increased slightly in the Asc-deficient mutant (Fig. 3D). The transition from state I to state II would decrease the 684/710 nm ratio; therefore, in our cultures grown at moderate light in TAP medium and subjected to strong red illumination during the fluorescence measurement, qT is unlikely to contribute to NPQ induction. On the other hand, when the actinic illumination was switched off, the 684/710 nm ratio decreased moderately, reflecting the occurrence of the state I-to-state II transition in the dark.

To further study the effect of state transition in the induction and relaxation of NPQ, we employed a state transition mutant, *stt7-9* (Depège et al., 2003). NPQ was induced during illumination in the *stt7-9* mutant to a similar extent as in the *Crvtc2-1* mutant (albeit with rather different kinetics), which coincided with a strong zeaxanthin accumulation (Supplemental Fig. S6B); this indicates that the transition to state II did not play a role in the formation of NPQ under the present experimental conditions. On the other hand, upon the cessation of actinic illumination, there was a rapid NPQ relaxation in the *stt7-9* mutant, showing that transition to state II occurs in the wild type and the *Crvtc2-1* mutant in the dark, probably masking the relaxation of the other NPQ components.

As a next step, the effect of oxidative stress, known to enhance NPQ (Roach and Na, 2017), was tested by employing H_2O_2 and catalase treatments on the *Crvtc2-1* mutant and its wild type. Figure 5, A and B, shows that upon addition of 1.5 mM H_2O_2, the slow NPQ component increased remarkably in both strains, without altering the de-epoxidation level (Fig. 5C). When 5 μg/mL catalase was added, NPQ was only slightly affected in the wild type (Fig. 5D), whereas it significantly decreased in the Asc-deficient mutant (Fig. 5E). These data suggest that H_2O_2 accumulated upon strong illumination in the Asc-deficient mutant, resulting in enhanced NPQ. On the other hand, the F_V/F_M value, an indicator of photosynthetic efficiency, did recover following illumination and to a similar extent in the wild type and the *Crvtc2-1* strain (Fig. 3C); thus, photosynthetic reaction centers were not severely inhibited.

For comparison, we also tested the *npq1* mutant lacking the CVDE enzyme, which was thus unable to perform violaxanthin de-epoxidation (Niyogi et al., 1997). Upon illumination with 530 μmol photons m^{-2} s^{-1}, this strain developed a large NPQ (Fig. 6A), which was accompanied by an irreversible decrease of F_V/F_M and loss of Chl and β-carotene relative to its wild type (137a) strain (Fig. 6, B–D). Fluorescence recordings at 77 K showed no changes in the 684/710 nm ratio (Fig. 6E); thus, the large NPQ component could be unambiguously attributed to qI. Interestingly, the Asc concentration in the *npq1* mutant was very high compared to that of the other strains (Fig. 6F), probably to compensate for the lack of CVDE and zeaxanthin in ROS management (Baroli et al., 2003). Thus, the experiments on the *npq1* mutant corroborate the importance of CVDE in strong illumination.

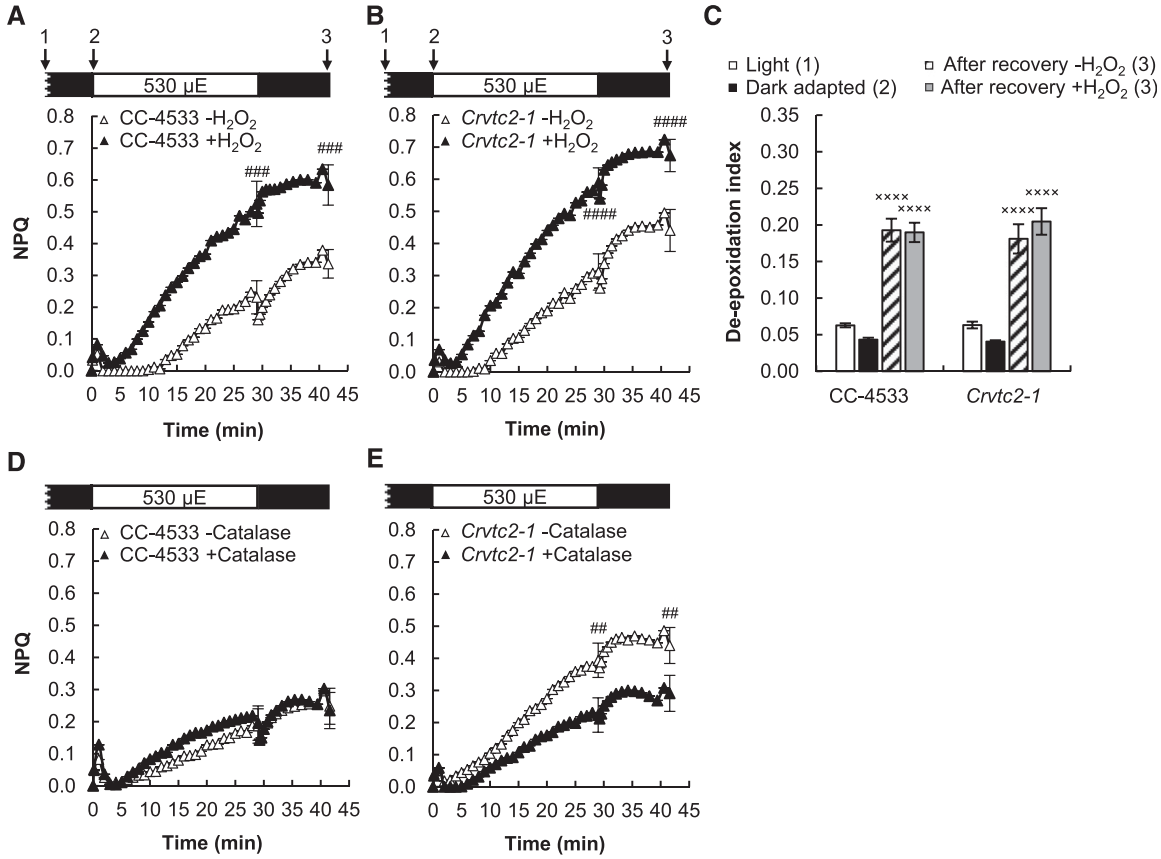

Figure 5. The effects of H_2O_2 and catalase on NPQ induced by strong red light (530 μmol photons m^{-2} s^{-1}) in the wild type (CC-4533) and the *Crvtc2-1* mutant grown in photomixotrophic conditions in TAP medium at 100 μmol photons m^{-2} s^{-1}. A, Effect of 1.5 mM H_2O_2 on NPQ induction in the CC-4533 strain. B, Effect of 1.5 mM H_2O_2 on NPQ induction in the *Crvtc2-1* mutant. C, Effect of H_2O_2 addition on de-epoxidation. D, Effect of catalase on NPQ induction in the CC-4533 strain. E, Effect of catalase on NPQ induction in the *Crvtc2-1* mutant. Samples were collected at the time points indicated by arrows in the schemes in A and B. The presented data are based on three independent experiments. When applicable, averages and SEs (±SE) were calculated. Data were analyzed by one-way ANOVA followed by Dunnett's posttest: ##, $P < 0.01$, ###, $P < 0.001$, and ####, $P < 0.0001$, compared to the untreated CC-4533 culture at the respective time point; ×, $P < 0.05$, ××, $P < 0.01$, and ×××, $P < 0.001$, compared to the dark-adapted CC-4533 strain. μE, μmol photons m^{-2} s^{-1}.

Effects of Asc Deficiency on NPQ in Cultures Grown under Photoautotrophic Conditions at High and Moderate Light

When the cultures were grown under photoautotrophic conditions without CO_2 supplementation under strong white light (530 μmol photons m^{-2} s^{-1}), which was similar in intensity to that used for NPQ induction measurements, qE reached relatively high values (~1.0) in both the wild type and the Asc-deficient CLiP mutant (Fig. 7A). In the *VTC2*-amiRNA line, the qE component was enhanced relative to its empty vector control (Supplemental Fig. S4D). These results show that Asc is not required for the formation of the qE component. The qE phase was followed by a slower one, which was enhanced in both the *Crvtc2-1* mutant and the *VTC2* amiRNA line relative to their control strains.

During illumination, the de-epoxidation index changed only marginally, and it was essentially the same in the wild type and the Asc-deficient strain (~0.1; Fig. 7B). The F_V/F_M value was also unaffected in the *Crvtc2-1* mutant relative to its wild type before and after illumination with strong red light (Fig. 7C). The 684/710 nm ratio of the 77 K spectra remained constant in the Asc-deficient mutant (Fig. 7D). The violaxanthin, antheraxanthin, zeaxanthin, and lutein contents did not decrease upon illumination with intense red light in either strain (Supplemental Fig. S7); only the total amount of β-carotene was slightly lower in the Asc-deficient mutant (Supplemental Fig. S7D). We also observed that under high light growth conditions, the amount of photosynthetic complexes (namely PsbA, CP43, PSBO, PsaA, LHCSR3, PetB, and RbcL) were essentially the same in the *Crvtc2-1* mutant and the wild type, as detected by immunoblot analysis on equal Chl basis (Supplemental Fig. S3).

Treatments with 1.5 mM H_2O_2 led to alteration of the NPQ kinetics and a slower relaxation in both strains (Fig. 8, A and B). In the *Crvtc2-1* mutant, catalase treatment resulted in a strong decrease of qE and the

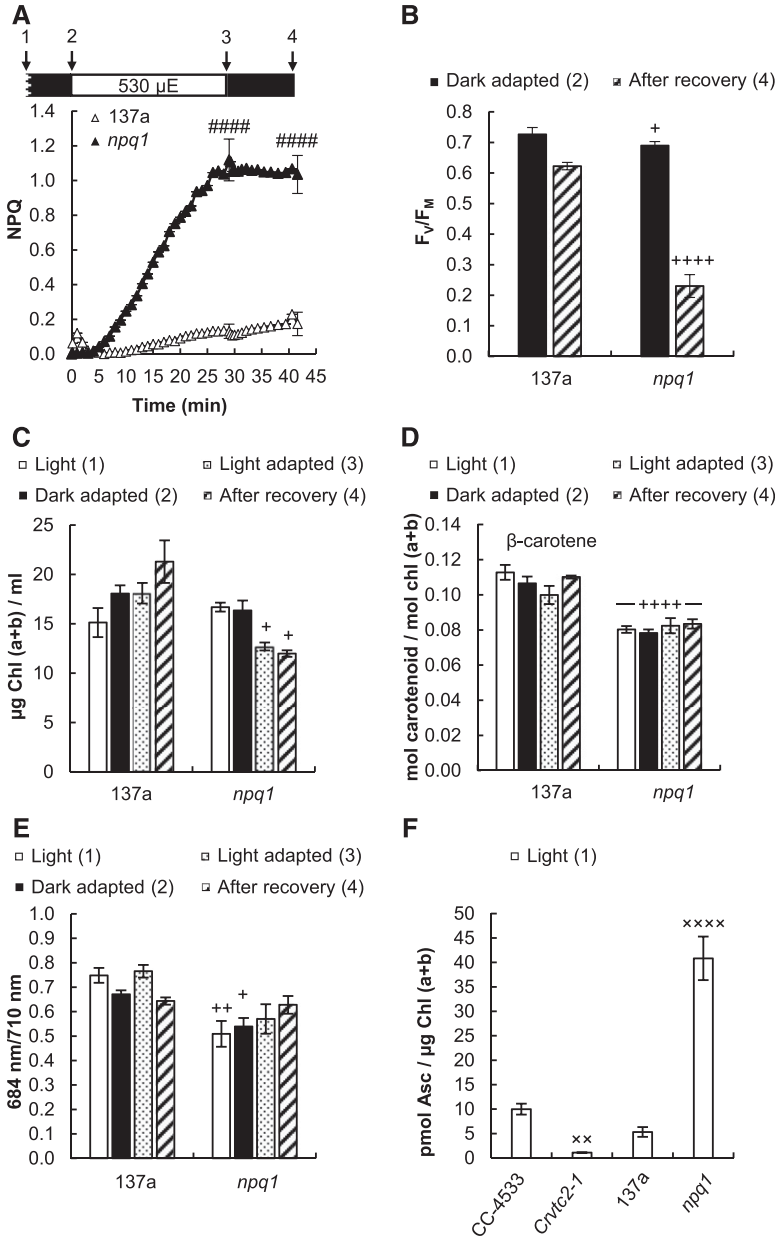

Figure 6. Effects of strong red light (530 μmol photons m^{-2} s^{-1}) on the 137a wild type and the *npq1* mutant of *C. reinhardtii* grown in TAP medium at 100 μmol photons m^{-2} s^{-1}. A, NPQ induced by 530 μmol photons m^{-2} s^{-1} of red light followed by a recovery phase. μE, μmol photons m^{-2} s^{-1}. B, F_V/F_M values determined before the strong red light illumination and after the recovery phase. C, Chl(*a*+*b*) content of the cultures determined before, during, and after the strong red light illumination. D, β-carotene content measured before, during, and after the strong red light illumination. E, The 684/710 nm ratio of the 77 K fluorescence spectra determined before, during, and after the strong red light illumination. F, Ascorbate contents of the *npq1* and *Crvtc2-1* mutants and the CC-4533 and 137a wild-type strains. Samples were collected at the time points indicated by arrows in the scheme in A. The presented data are based on five independent experiments. When applicable, averages and SES (±SE) were calculated. Data were analyzed by one-way ANOVA followed by Dunnett's posttest: ####, $P < 0.0001$ (A) compared to the 137a strain at the respective time point; +, $P < 0.05$, ++, $P < 0.01$, and ++++, $P < 0.0001$ (C–E), compared to the dark-adapted 137a strain; ××, $P < 0.01$, and ××××, $P < 0.0001$ (F), compared to the CC-4533 strain.

slow NPQ component (Fig. 8, C and D). These results show that under photoautotrophic and high light conditions, Asc deficiency does not limit qE or qZ but may lead to the occurrence of oxidative stress and thereby to increased qI.

Subjecting the cells in HS medium to moderate light (100 μmol photons m^{-2} s^{-1}) resulted in similar effects in terms of qE, de-epoxidation, the 684/710 nm ratio of the 77 K spectra, and H_2O_2 and catalase responsiveness (Supplemental Fig. S8).

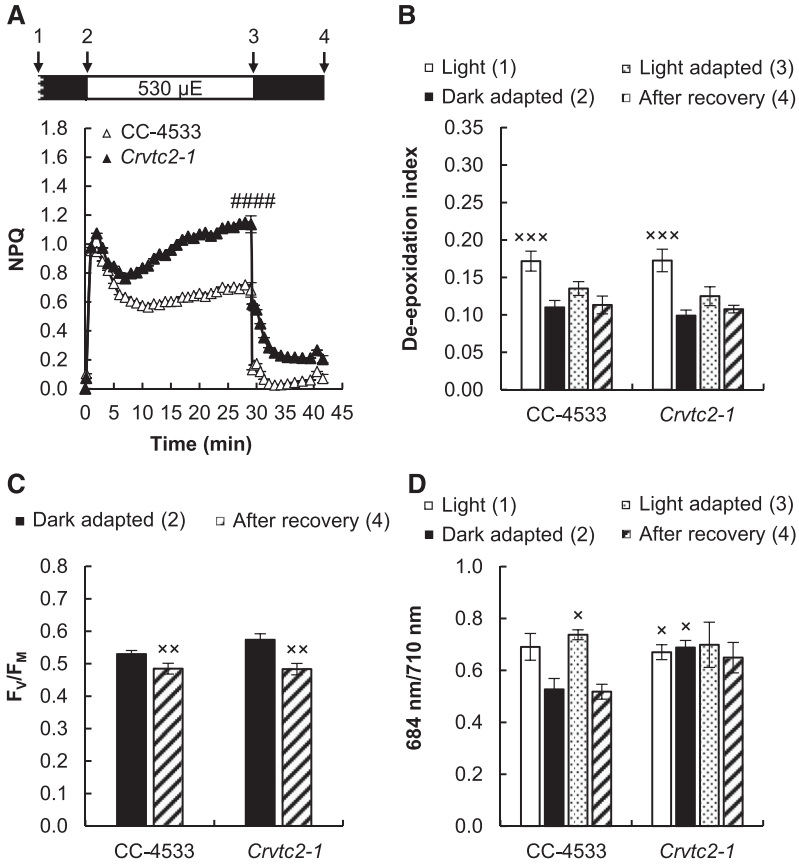

Figure 7. Acclimation to 530 μmol photons m^{-2} s^{-1} of red light followed by recovery in CC-4533 and *Crvtc2-1* cultures grown photoautotrophically in HS medium at 530 μmol photons m^{-2} s^{-1}. A, NPQ kinetics. Data were analyzed by one-way ANOVA followed by Dunnett's posttest: ####, $P < 0.0001$, compared to the CC-4533 strain at the respective time poin. μE, μmol photons m^{-2} s^{-1}. B, De-epoxidation index. C, F_V/F_M parameter measured after dark adaptation and after recovery from the 530 μmol photons m^{-2} s^{-1} red light illumination. D, The 684/710 nm ratio of the 77 K fluorescence spectra. The samples were collected at the growth light of 530 μmol photons m^{-2} s^{-1}, after 30 min of dark adaptation, at the end of the 30 min red light illumination, and 12 min after the cessation of actinic illumination, as indicated in the scheme in A. The presented data are based on eight independent experiments. When applicable, averages and SES (±SE) were calculated. Data were analyzed by one-way ANOVA followed by Dunnett's posttest:×, $P < 0.05$, ××, $P < 0.01$, and ×××, $P < 0.001$, compared to the dark-adapted CC-4533 strain.

DISCUSSION

The *Crvtc2-1* CLiP Mutant Possesses a Low Asc Content without Major Changes in the Phenotype

VTC2 encodes GDP-L-Gal phosphorylase, an essential and highly regulated enzyme of Asc biosynthesis both in vascular plants and in green algae (Urzica et al., 2012; Vidal-Meireles et al., 2017), and down-regulating *VTC2* via the amiRNA technique results in Asc deficiency (Vidal-Meireles et al., 2017). For the current study, we identified and genetically complemented a *VTC2* mutant in the CLiP collection that carries a single insertion in the *VTC2* gene (Figs. 1 and 2). Asc content in the *Crvtc2-1* mutant was ~10% of that in its wild-type strain, CC-4533, under normal growth conditions; was unaltered upon H_2O_2 treatment; and remained <20% of the wild-type content under high light conditions. In addition, employing overnight dark acclimation caused the Asc concentration of the *Crvtc2-1* mutant to strongly decrease (Fig. 4).

The *Crvtc2-1* mutant is likely a knockout for *VTC2*, as no transcript accumulation was detected when performing RT-PCR with primers annealing downstream of the CIB cassette insertion site and spanning the sequence encoding the catalytic site of GDP-L-Gal phosphorylase. A faint band could only be observed in the gel when the cultures were treated with H_2O_2 and when a high PCR cycle number was used (Fig. 1E). It is very unlikely that a functional truncated GDP-L-Gal phosphorylase is present in the mutant, but the observation that the *Crvtc2-1* strain still contains 10% to 20% Asc relative to its parent strain suggests that some phosphorolysis of GDP-L-Gal could be carried out by another enzyme, ensuring a minor amount of Asc. We note that in Arabidopsis, *VTC2* has a weakly expressed homolog, *VTC5*, and knocking out both of them results

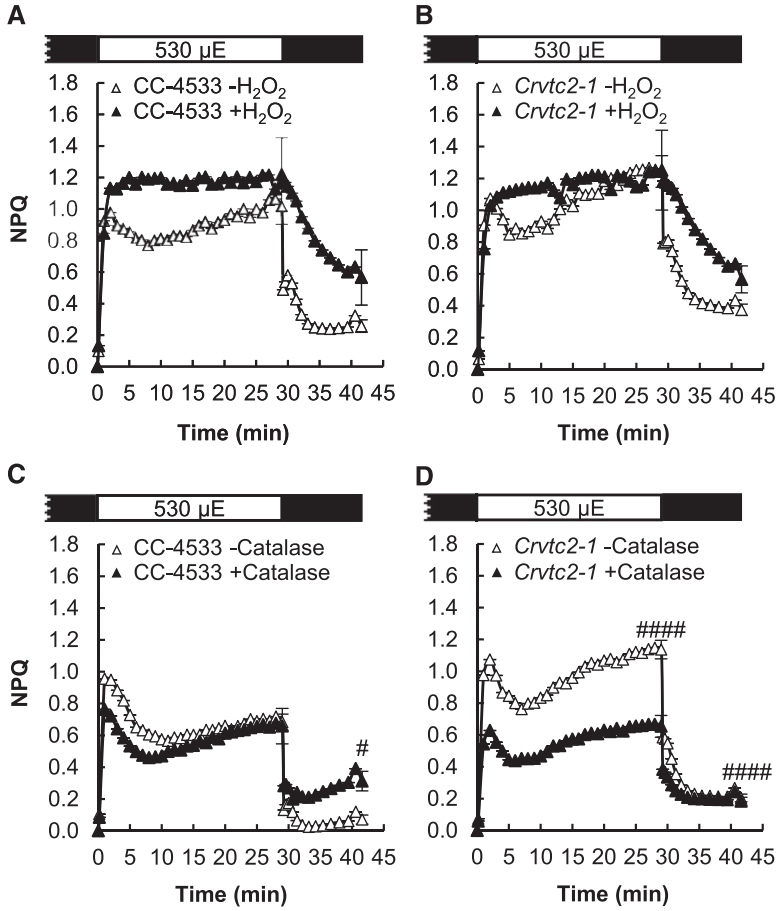

Figure 8. The effects of H_2O_2 and catalase on NPQ induced by strong red light (530 μmol photons m^{-2} s^{-1}) in the wild-type (CC-4533) and *Crvtc2-1* mutant strains grown photoautotrophically in HS medium at 530 μmol photons m^{-2} s^{-1}. A, Effect of 1.5 mM H_2O_2 on NPQ induction in the CC-4533 strain. B, Effect of 1.5 mM H_2O_2 on NPQ induction in the *Crvtc2-1* mutant. C, Effect of catalase on NPQ induction in the CC-4533 strain. D, Effect of catalase on NPQ induction in the *Crvtc2-1* mutant. The presented data are based on four independent experiments. When applicable, averages and SEs (±SE) were calculated. Data were analyzed by one-way ANOVA followed by Dunnett's posttest: #, $P < 0.05$, and ####, $P < 0.0001$, compared to the untreated CC-4533 culture at the respective time point. μE, μmol photons m^{-2} s^{-1}.

in seedling lethality (Dowdle et al., 2007). In *C. reinhardtii*, no homolog of *VTC2* has been identified (Urzica et al., 2012). On the other hand, it is possible that GDP-L-Gal is degraded hydrolytically (with L-Gal-1-P and GMP as products), leading to minor Asc production in the *VTC2* mutant. An alternative Asc biosynthesis pathway may also exist in *C. reinhardtii*, although homologs of enzymes possibly involved in alternative Asc biosynthesis pathways in vascular plants could not be found in *C. reinhardtii* (Urzica et al., 2012; Wheeler et al., 2015).

In spite of the very low Asc content of the *Crvtc2-1* mutant, the phenotype was only slightly affected. The *Crvtc2-1* mutant had the same growth rate as the wild type and the complementation lines under moderate light conditions in TAP medium (Supplemental Fig. S2). The amounts of various photosynthetic subunits were similar between the Asc-deficient *Crvtc2-1* mutant and the wild-type strain CC-4533 in TAP medium at moderate light and also in HS medium at both moderate and high light (Supplemental Fig. S3). Unexpectedly, the amount of the photoprotective LHCSR3 protein was reduced in the *Crvtc2-1* mutant in TAP medium at moderate light and was the same level as in the wild type when grown in HS medium both at medium and high light. The amounts of carotenoids were unchanged in the *Crvtc2-1* line in cultures grown at normal light, whereas at high light in HS medium, the amount of β-carotene was slightly reduced (Supplemental Figs. S5 and S7). The *Crvtc2-1* line had a slightly higher Chl content and moderately larger cell size than its wild type (Fig. 2). A marked characteristic of the *Crvtc2-1* mutants was that it was unable to grow at high light in TAP medium (Supplemental Fig. S2).

In our previously published *VTC2*-amiRNA line, Asc deficiency led to more severe alterations in the phenotype than were observed in the *Crvtc2-1* mutant (Vidal-Meireles et al., 2017). The reason behind this remains to be elucidated, although the cell wall deficiency of the cw15-325 line (the parent strain of the

VTC2-amiRNA line), and thereby its increased stress sensitivity (Voigt and Münzner, 1994), may explain the differences between the *VTC2*-amiRNA and *Crvtc2-1* insertional mutant strains.

Effects of Asc Deficiency on the qE Component of NPQ

C. reinhardtii uses various photoacclimation strategies, which strongly depend on carbon availability and trophic status of the cells (Polukhina et al., 2016). The fast rise in NPQ (qE) is enhanced upon growth at high light and low CO_2 enabled by a high expression of LHCSR3 (e.g. Peers et al., 2009). Under photomixotrophic conditions at normal light, the expression of the LHCSR proteins is very low and qE is minor; in addition, the de-epoxidation state also varies with the growth light (Polukhina et al., 2016). Therefore, to study the role of Asc in the different NPQ parameters, we subjected the cultures to both moderate and high light, and both photomixotrophic and photoautotrophic conditions. As shown by our results and the discussion below, by these means we managed to distinguish between qE, qZ, and qI; only qT could not be studied in detail.

Rapid response to changes in light intensity and dissipation of excess light energy are particularly important when the activity of the Calvin-Benson-Bassham cycle is limiting, to avoid a potentially deleterious buildup of excessive ΔpH (Kanazawa and Kramer, 2002; Takizawa et al., 2008). In agreement with the literature (Xue et al., 2015), at normal light and photomixotrophic conditions, the rapidly inducible qE was a minor component and the relative amount of the LHCSR3 protein, essential for qE development, was low (Supplemental Fig. S3). When *C. reinhardtii* cultures were grown at photoautotrophic, possibly CO_2-limiting conditions, the amplitude of qE largely increased at both moderate (Supplemental Fig. S8) and high light (Fig. 8) enabled by the accumulation of LHCSR3 (Supplemental Fig. S3) and possibly by other factors.

Our results for the *Crvtc2-1* line show that qE is not limited by Asc deficiency either at low or high light conditions, or under photomixotrophic or photoautotrophic conditions; in the *VTC2*-amiRNA line, qE was even enhanced relative to its control line (Supplemental Fig. S4B).

Effects of Asc Deficiency on the Slow NPQ Components

In *C. reinhardtii*, a slow NPQ component, with several underlying mechanisms, may also be induced. When CC-4533 cultures were grown at normal light in TAP medium and subjected to strong red light, the major slow component was probably qZ, as shown by the large increase in de-epoxidation (Fig. 3) and by the loss of NPQ induction in the *npq1* mutant (Fig. 6). In cultures grown at high light and photoautotrophic conditions, de-epoxidation was minor upon light adaptation with strong red light (Fig. 7) and intermediate when the cultures were grown photoautotrophically at moderate light (Supplemental Fig. S8). De-epoxidation was equal in the *Crvtc2-1* mutant and the wild type in all growth conditions and also upon overnight dark acclimation that led to undetectably low Asc content in the *Crvtc2-1* mutant. These results clearly show that Asc deficiency does not limit qZ; thus, Asc is not used as a reductant by CrCVDE.

The xanthophyll cycle, in which violaxanthin is converted into zeaxanthin during light acclimation, is ubiquitous among green algae, mosses, and plants, with the exception of Bryopsidales, a monophyletic branch of Ulvophyceae in which NPQ is neither related to a pH-dependent mechanism nor modulated by the activity of the xanthophyll cycle (Christa et al., 2017). Among green alga species, large variations exist in the activity of the xanthophyll cycle and in its overall contribution to NPQ, which seems to depend on environmental selection pressure and less on phylogeny (Quaas et al., 2015). In mosses, the xanthophyll cycle significantly contributes to excess energy dissipation under stress conditions (e.g. Azzabi et al., 2012).

The de-epoxidation reaction itself is catalyzed by distinct enzymes in vascular plants and in Chlorophyceae, including *C. reinhardtii* (Li et al., 2016a). Plant-type VDE is associated with the thylakoid membrane on the luminal side, where it catalyzes the de-epoxidation reaction of violaxanthin, found in free lipid phase, and uses Asc as a reductant (Hager and Holocher, 1994; Arnoux et al., 2009). CVDE is located on the stromal side of the thylakoid membrane, and just like vascular plant VDE, it also requires a build-up of ΔpH for its activity (Li et al., 2016a). CVDE is related to lycopene cyclases of photosynthetic bacteria, called CruA and CruP (Li et al., 2016a; Bradbury et al., 2012). We have demonstrated in this work that Asc is not required for the de-epoxidation reaction or, in general, for qZ in *C. reinhardtii*.

Green algae contain very small amounts of Asc relative to vascular plants, and, as stated above, effective de-epoxidation is achieved by an enzyme that does not require Asc as a reductant. Interestingly, in brown algae, which produce minor amounts of Asc as well, diadinoxanthin de-epoxidase uses Asc as a reductant with much higher affinity for Asc than plant-type VDE, in combination with a shift of its pH optimum toward lower values, enabling efficient de-epoxidation (Grouneva et al., 2006). Mosses have plant-type VDE enzymes (Pinnola et al., 2013), which probably require Asc as a reductant. Since mosses contain ~10 times less Asc compared to vascular plants (Gest et al., 2013), it remains to be explored how this low amount of Asc allows a rapid and intensive development of NPQ, characteristic of mosses (e.g. Marschall and Proctor, 2004).

In *C. reinhardtii*, light- and oxygen-availability-dependent state transitions (qT) involving major reorganization of LHCs also modulate NPQ (Depège et al., 2003; Lemeille et al., 2009; Ünlü et al., 2014). Under

our experimental conditions, ensuring aeration during both dark and light adaptation and using strong red light as actinic light, no decrease occurred in the 685/710 nm ratio of the 77 K fluorescence spectra, suggesting that the state I-to-state II transition did not affect NPQ induction in the wild type or the Asc-deficient strains. The *stt7-9* mutant, which is unable to perform the state transition, did not show decreased NPQ (Supplemental Fig. S6), which would be expected if state transition constituted a major form of NPQ under our experimental conditions. However, our data do not exclude the possibility that Asc may participate in the state transition under conditions favoring its occurrence.

A fourth and rather complex component of NPQ is qI, possibly with several underlying mechanisms involved (Adams et al., 2013; Tikkanen et al., 2014). We observed both under photomixotrophic conditions at moderate light and under photoautotrophic conditions that the slow NPQ component was enhanced in the *Crvtc2-1* mutant upon illumination with strong red light, which was not attributable to qZ or qT. Asc deficiency is accompanied by an increase in the intracellular H_2O_2 content in *C. reinhardtii* (Vidal-Meireles et al., 2017), and ROS are known to enhance NPQ via several mechanisms (Roach and Na, 2017). Using H_2O_2 and catalase treatments (Figs. 5 and 8; Supplemental Fig. S8), we clearly show that ROS formation is involved in the slowly induced NPQ component in the Asc-deficient strain, which can be interpreted as qI. In the wild type, the contribution of qI to NPQ was probably minor under our experimental conditions, since catalase treatment did not diminish NPQ formation (Fig. 5D).

In conclusion, our results reveal fundamental differences between vascular plants and *C. reinhardtii* regarding the role of Asc in NPQ. Whereas the most prominent role of Asc in vascular plants is as a reductant of VDE, it is pertinent in preventing ROS formation that would lead to qI mechanisms in *C. reinhardtii*.

MATERIALS AND METHODS

Algal Strains and Growth Conditions

Chlamydomonas reinhardtii strains CC-4533 (designated as wild type) and LMJ.RY0402.058624 (designated as *Crvtc2-1* mutant) were obtained from the CLiP library (Li et al., 2016b). The 137a (CC-125) strain and the *npq1* (CC-4100) mutant were obtained from the *Chlamydomonas* Resource Center (https://www.chlamycollection.org/). The *ARG7* complemented strain *cw15-412*, provided by Dr. Michael Schroda (Technische Universität Kaiserslautern, Kaiserslautern, Germany), was used as control for the *stt7-9* mutant (Depège et al., 2003). The *VTC2*-amiRNA strain and its control *EV2* strain are described in Vidal-Meireles et al. (2017).

The synthetic coding sequence of *VTC2*, including a 38 bp-long upstream sequence homologous to the *PSAD* 5′ UTR with the BsmI restriction enzyme recognition site was ordered from Genecust (www.genecust.com). The *VTC2* insert was ligated as BsmI/*Eco*RI fragment into the similarly digested pJR39 (Neupert et al., 2009) vector, resulting in vector pJR112. Finally, pJR112 was digested with BsmI and *Sma*I, and the *VTC2*-containing BsmI/*Sma*I fragment was ligated to the similarly digested pJR91 vector that carries the *APH7″* resistance marker for selection on hygromycin-B. Transformation of the *Crvtc2-1* mutant strain was done via electroporation in a Bio-Rad GenePulser Xcell instrument, at 1,000 V, with 10 F capacitance and infinite resistance using a 4-mm gap cuvette. The cells were plated onto selective agar plates (TAP + 10 μg/mL hygromycin-B), and colonies were picked after 10 d of growth under moderate light (80 μmol photons m^{-2} s^{-1}).

C. reinhardtii precultures were grown in 50-mL Erlenmeyer flasks in TAP medium for 3 d at 22°C and 100 μmol photons m^{-2} s^{-1} on a rotatory shaker. Following this phase, cultures were grown in 100-mL Erlenmeyer flasks photomixotrophically (in TAP medium) or photoautotrophically (in HS medium) at 22°C at 100 or 530 μmol photons m^{-2} s^{-1} for an additional 2 d. The initial cell density was set to 1 million cells/mL.

DNA Isolation and PCR

Total genomic DNA from *C. reinhardtii* strains CC-4533 and *Crvt2-1* (LMJ.RY0402.058624) was extracted according to published protocols (Schroda et al., 2001; Barahimipour et al., 2015), and 1 μL of the extracted DNA was used as a template for the PCR assays, using GoTaq DNA polymerase (Promega GmbH).

To confirm the CIB1 insertion site in the *Crvt2-1* strain, PCR assays were conducted using gene-specific primers that anneal upstream and downstream of the predicted insertion site of the cassette, as well as primers specific for the 5′ and 3′ ends of the CIB cassette. Primers 1 (5′-TGATGGCCAAGGGCTTAGTG-3′) and 2 (5′-CCGCAAACACCATGCAATCT-3′) amplified the region of the gene upstream of the predicted site of CIB1 cassette insertion (control amplicon with an expected size of 852 bp); primers 3 (5′-AGATTGCATGGTGTTTGCGG-3′) and 4 (5′-CAGGCCATGTGAGAGTTTGCC-3′) amplified the 3′ junction site of the CIB1 cassette (amplicon with an expected size of 470 bp); and primers 5 (5′-GCACCAATCATGTCAAGCCT-3′) and 6 (5′-TGTTGTAGCCCACGC GGAAG-3′) amplified the 5′ junction site of the cassette (amplicon with an expected size of 601 bp). Primers 11 (5′-GCTCTTGACTCGTTGTGCATTCTA G-3′) and 12 (5′-CACTGAGACACGTCGTACCTG-3′) amplified the 3′ junction site of the *PsaD* promoter with the *VTC2* gene in the plasmid used for complementation (amplicon with an expected size of 841 bp).

Analyses of Gene Expression

Sample collection and RNA isolation were performed as in Vidal-Meireles et al., (2017). The primer pairs for the *VTC2* gene and the reference genes (*bTub2* [Cre12.g549550], *actin* [Cre13.g603700], and *UBQ* [XP_001694320]) used in RT-qPCR were published earlier in Vidal-Meireles et al. (2017). The annealing sites for analyzing *VTC2* expression are indicated as primers 7 and 8 in Figure 1. RT-PCR products using primers 9 (5′-AACCACCTGCACTTCCACGCTTAC-3′) and 10 (5′-TGCCCCGCAATCTCAAACGATG-3′), which span the sequence encoding the catalytic site of *VTC2* (amplicon with an expected size of 434 bp), were analyzed by electrophoresis.

The RT-qPCR data are presented as the fold change in mRNA transcript abundance of *VTC2* normalized to the average of the three reference genes and relative to the untreated CC-4533 strain. RT-qPCR analysis was carried out with three technical replicates for each sample, and three biological replicates were measured; the SE was calculated based on the range of fold change by calculating the minimum and the maximum of the fold change using the SDS of $\Delta\Delta$Ct.

Determination of Cell Size, Cell Density, Chlorophyll, Asc and Carotenoid Contents

The cell density was determined by a Scepter 2.0 hand-held cell counter (Millipore), as described in Vidal-Meireles et al., (2017). Chl content was determined according to Porra et al. (1989), and the Asc content was determined as in Kovács et al., (2016). For carotenoid content determination, liquid culture containing 30 μg Chl(a+b)/mL was filtered onto a Whatman glass microfiber filter (GF/C) and frozen in liquid N_2 at different time points in the NPQ induction protocol. The pigments were extracted by resuspending the cells in 500 μL of ice-cold acetone. After resuspension, the samples were incubated in the dark for 30 min. This was followed by centrifugation at 11,500g, 4°C, for 10 min, and the supernatant was collected and passed through a PTFE 0.2-μm pore size syringe filter.

Quantification of carotenoids was performed by HPLC using a Shimadzu Prominence HPLC system consisting of two LC-20AD pumps, a DGU-20A degasser, a SIL-20AC automatic sample injector, a CTO-20AC column thermostat, and a Nexera X2 SPD-M30A photodiode-array detector. Chromatographic

separations were carried out on a Phenomenex Synergi Hydro-RP 250 × 4.6-mm column with a particle size of 4 μm and a pore size of 80 Å. Twenty-microliter aliquots of acetonic extract were injected into the column and the pigments were eluted by a linear gradient from solvent A (9:1:0.01 acetonitrile:water:triethylamine) to solvent B (ethyl acetate). The gradient from solvent A to solvent B was run from 0 to 25 min at a flow rate of 1 mL/min. The column temperature was set to 25°C. Eluates were monitored in a wavelength range of 260–750 nm at a sampling frequency of 1.5625 Hz. Pigments were identified according to their retention time and absorption spectrum and quantified by integrated chromatographic peak area recorded at the wavelength of maximum absorbance for each kind of pigment using the corresponding molar decadic absorption coefficient (Jeffrey et al., 1997). The de-epoxidation index of the xanthophyll cycle components was calculated as (zeaxanthin + antheraxanthin)/(violaxanthin + anteraxanthin + zeaxanthin).

Chemical Treatments

For Asc supplementation, 1 mM Na-Asc (Roth GmbH) was added to the cultures, and measurements were carried out after a 2-h incubation period in the light. For H_2O_2 treatments, the cell density was adjusted to 3 million cells/mL and 1.5 mM H_2O_2 (Sigma Aldrich) was added. The presented measurements were carried out 7 h following the addition of H_2O_2. Catalase (5 μg/mL, from bovine liver; Sigma Aldrich) was added after a 30-min dark adaptation, and the measurements were carried out after an additional 2-h incubation period in the dark with shaking.

Immunoblot Analysis

Protein isolation and immunoblot analysis were performed as in Vidal-Meireles et al. (2017). Specific polyclonal antibodies (produced in rabbits) against PsaA, PsbA, RbcL, LHCSR3, CP43, and PetB were purchased from Agrisera AB. Specific polyclonal antibody (produced in rabbits) against PSBO was purchased from AntiProt.

NPQ Measurements

Chlorophyll *a* fluorescence was measured using a Dual-PAM-100 instrument (Heinz Walz GmbH). *C. reinhardtii* cultures were dark adapted for 30 min; then, liquid culture containing 30 μg Chl(*a*+*b*)/mL was filtered onto Whatman glass microfiber filters (GF/B) that were placed between two microscopy coverslips with a spacer to allow for gas exchange. For NPQ induction, light adaptation consisted of 30 min illumination at 530 μmol photons m^{-2} s^{-1}, followed by 12 min of dark adaptation interrupted with saturating pulses of 3,000 μmol photons m^{-2} s^{-1}.

Low-Temperature Fluorescence Emission Spectra (77 K) Measurements

Algal cultures containing 2 μg Chl(*a*+*b*)/mL were collected at several time points during the NPQ induction protocol. Subsequently, the sample was filtered onto a Whatman glass microfiber filter (GF/C), placed in a sample holder, and immediately frozen in liquid nitrogen. Low-temperature (77 K) fluorescence emission spectra were measured using a spectrofluorometer (Fluorolog-3; Jobin-Yvon-Spex Instrument S.A.) equipped with a home-made liquid nitrogen cryostat. The fluorescence emission spectra between 650 and 750 nm were recorded with an interval of 0.5 nm, using an excitation wavelength of 436 nm and excitation and emission slits of 5 and 2 nm, respectively. The final spectra were corrected for the photomultiplier's spectral sensitivity.

Statistics

The presented data are based on at least three independent experiments. When applicable, averages and SES (±SE) were calculated. Statistical significance was determined using one-way ANOVA followed by Dunnett multiple comparison posttests (GraphPad Prism 7.04; GraphPad Software). Changes were considered statistically significant at $P < 0.05$.

Accession Numbers

The accession numbers for *C. reinhardtii* genes *VTC2*, *NPQ1* and *STT7* are Cre13.g588150, Cre09.g388060, and Cre02.g120250, respectively. The *Crvtc2-1* mutant strain from the CLiP library is LMJ.RY0402.058624.

Supplemental Data

The following supplemental materials are available.

Supplemental Figure S1. Confirmation of the location of the CIB1 casette in the insertional CLiP mutant of *C. reinhardtii* affected in the *VTC2* gene.

Supplemental Figure S2. Characterization of the CC-4533, *Crvtc2-1* mutant, and *Crvtc2-1*+*VTC2* complemented *C. reinhardtii* lines in terms of cell volume, Chl content, culture growth, and Asc content.

Supplemental Figure S3. Immunoblot analysis for the semiquantitative determination of PsbA, CP43, PSBO, PsaA, LHCSR3, PetB, and RbcL contents in *Crvtc2-1* and *npq1 C. reinhardtii* mutants.

Supplemental Figure S4. NPQ kinetics induced by strong red light in the *Crvtc2-1* mutant, the *Crvtc2-1*+*VTC2* complemented lines, and a *VTC2-amiRNA* line grown either in photomixotrophic conditions in TAP medium or in photoautotrophic conditions in HS medium.

Supplemental Figure S5. Carotenoid contents of the *Crvtc2-1* mutant and the wild type during NPQ induction by strong red light.

Supplemental Figure S6. NPQ induction in the *stt7-9* mutant of *C. reinhardtii* and in *cw15-412*.

Supplemental Figure S7. Carotenoid contents of the *Crvtc2-1* mutant and the wild type during NPQ induction upon strong red light.

Supplemental Figure S8. Acclimation to 530 μmol photons m^{-2} s^{-1} of red light followed by recovery in CC-4533 and *Crvtc2-1* cultures grown photoautotrophically in HS medium at 100 μmol photons m^{-2} s^{-1}.

ACKNOWLEDGMENTS

The authors thank Dr. Ralph Bock (Max-Planck Institut für Molekulare Pflanzenphysiologie, Potsdam, Germany) and Dr. Petar Lambrev (Biological Research Centre (BRC), Szeged, Hungary) for discussions, Dr. Anikó Galambos (BRC, Szeged, Hungary) for assistance with ordering the mutants from the CLiP library, and Dr. László Szabados (BRC, Szeged, Hungary) for use of their Fusion FX5 (Vilber Lourmat) camera.

Received July 25, 2019; accepted October 21, 2019; published October 29, 2019.

LITERATURE CITED

Adams WW III, Muller O, Cohu CM, Demmig-Adams B (2013) May photoinhibition be a consequence, rather than a cause, of limited plant productivity? Photosynth Res **117:** 31–44

Allorent G, Tokutsu R, Roach T, Peers G, Cardol P, Girard-Bascou J, Seigneurin-Berny D, Petroutsos D, Kuntz M, Breyton C, et al (2013) A dual strategy to cope with high light in *Chlamydomonas reinhardtii*. Plant Cell **25:** 545–557

Arnoux P, Morosinotto T, Saga G, Bassi R, Pignol D (2009) A structural basis for the pH-dependent xanthophyll cycle in *Arabidopsis thaliana*. Plant Cell **21:** 2036–2044

Asada K (2006) Production and scavenging of reactive oxygen species in chloroplasts and their functions. Plant Physiol **141:** 391–396

Avenson TJ, Ahn TK, Zigmantas D, Niyogi KK, Li Z, Ballottari M, Bassi R, Fleming GR (2008) Zeaxanthin radical cation formation in minor light-harvesting complexes of higher plant antenna. J Biol Chem **283:** 3550–3558

Azzabi G, Pinnola A, Betterle N, Bassi R, Alboresi A (2012) Enhancement of non-photochemical quenching in the Bryophyte *Physcomitrella patens* during acclimation to salt and osmotic stress. Plant Cell Physiol **53:** 1815–1825

Barahimipour R, Strenkert D, Neupert J, Schroda M, Merchant SS, Bock R (2015) Dissecting the contributions of GC content and codon usage to

gene expression in the model alga *Chlamydomonas reinhardtii*. Plant J **84:** 704–717

Baroli I, Do AD, Yamane T, Niyogi KK (2003) Zeaxanthin accumulation in the absence of a functional xanthophyll cycle protects *Chlamydomonas reinhardtii* from photooxidative stress. Plant Cell **15:** 992–1008

Bratt CE, Arvidsson PO, Carlsson M, Akerlund HE (1995) Regulation of violaxanthin de-epoxidase activity by pH and ascorbate concentration. Photosynth Res **45:** 169–175

Bonente G, Ballottari M, Truong TB, Morosinotto T, Ahn TK, Fleming GR, Niyogi KK, Bassi R (2011) Analysis of LhcSR3, a protein essential for feedback de-excitation in the green alga *Chlamydomonas reinhardtii*. PLoS Biol **9:** e1000577

Bradbury LMT, Shumskaya M, Tzfadia O, Wu S-B, Kennelly EJ, Wurtzel ET (2012) Lycopene cyclase paralog CruP protects against reactive oxygen species in oxygenic photosynthetic organisms. Proc Natl Acad Sci USA **109:** E1888–E1897

Chaux F, Johnson X, Auroy P, Beyly-Adriano A, Te I, Cuiné S, Peltier G (2017) PGRL1 and LHCSR3 compensate for each other in controlling photosynthesis and avoiding photosystem I photoinhibition during high light acclimation of *Chlamydomonas* cells. Mol Plant **10:** 216–218

Christa G, Cruz S, Jahns P, de Vries J, Cartaxana P, Esteves AC, Serôdio J, Gould SB (2017) Photoprotection in a monophyletic branch of chlorophyte algae is independent of energy-dependent quenching (qE). New Phytol **214:** 1132–1144

Depège N, Bellafiore S, Rochaix JD (2003) Role of chloroplast protein kinase Stt7 in LHCII phosphorylation and state transition in *Chlamydomonas*. Science **299:** 1572–1575

Dowdle J, Ishikawa T, Gatzek S, Rolinski S, Smirnoff N (2007) Two genes in *Arabidopsis thaliana* encoding GDP-L-galactose phosphorylase are required for ascorbate biosynthesis and seedling viability. Plant J **52:** 673–689

Erickson E, Wakao S, Niyogi KK (2015) Light stress and photoprotection in *Chlamydomonas reinhardtii*. Plant J **82:** 449–465

Finazzi G, Johnson GN, Dall'Osto L, Zito F, Bonente G, Bassi R, Wollman F-A (2006) Nonphotochemical quenching of chlorophyll fluorescence in *Chlamydomonas reinhardtii*. Biochemistry **45:** 1490–1498

Foyer CH, Shigeoka S (2011) Understanding oxidative stress and antioxidant functions to enhance photosynthesis. Plant Physiol **155:** 93–100

Gest N, Gautier H, Stevens R (2013) Ascorbate as seen through plant evolution: The rise of a successful molecule? J Exp Bot **64:** 33–53

Grouneva I, Jakob T, Wilhelm C, Goss R (2006) Influence of ascorbate and pH on the activity of the diatom xanthophyll cycle-enzyme diadinoxanthin de-epoxidase. Physiol Plant **126:** 205–211

Hager A, Holocher K (1994) Localization of the xanthophyll-cycle enzyme violaxanthin de-epoxidase within the thylakoid lumen and abolition of its mobility by a (light-dependent) pH decrease. Planta **192:** 581–589

Hallin EI, Hasan M, Guo K, Åkerlund H-E (2016) Molecular studies on structural changes and oligomerisation of violaxanthin de-epoxidase associated with the pH-dependent activation. Photosynth Res **129:** 29–41

Holt NE, Zigmantas D, Valkunas L, Li X-P, Niyogi KK, Fleming GR (2005) Carotenoid cation formation and the regulation of photosynthetic light harvesting. Science **307:** 433–436

Holub O, Seufferheld MJ, Gohlke C, Govindjee, Heiss GJ, Clegg RM (2007) Fluorescence lifetime imaging microscopy of *Chlamydomonas reinhardtii*: Non-photochemical quenching mutants and the effect of photosynthetic inhibitors on the slow chlorophyll fluorescence transient. J Microsc **226:** 90–120

Ivanov B, Asada K, Edwards GE (2007) Analysis of donors of electrons to photosystem I and cyclic electron flow by redox kinetics of P700 in chloroplasts of isolated bundle sheath strands of maize. Photosynth Res **92:** 65–74

Iwai M, Kato N, Minagawa J (2007) Distinct physiological responses to a high light and low CO_2 environment revealed by fluorescence quenching in photoautotrophically grown *Chlamydomonas reinhardtii*. Photosynth Res **94:** 307–314

Jeffrey SW, Mantoura RFC, Wright SW (1997) Phytoplankton Pigments in Oceanography: Guidelines to Modern Methods. UNESCO Publishing, Paris

Johnson X, Alric J (2012) Interaction between starch breakdown, acetate assimilation, and photosynthetic cyclic electron flow in *Chlamydomonas reinhardtii*. J Biol Chem **287:** 26445–26452

Johnson MP, Davison PA, Ruban AV, Horton P (2008) The xanthophyll cycle pool size controls the kinetics of non-photochemical quenching in *Arabidopsis thaliana*. FEBS Lett **582:** 262–266

Kanazawa A, Kramer DM (2002) In vivo modulation of nonphotochemical exciton quenching (NPQ) by regulation of the chloroplast ATP synthase. Proc Natl Acad Sci USA **99:** 12789–12794

Kovács L, Vidal-Meireles A, Nagy V, Tóth SZ (2016) Quantitative determination of ascorbate from the green alga *Chlamydomonas reinhardtii* by HPLC. Bio Protoc **6:** e2067

Lemeille S, Willig A, Depège-Fargeix N, Delessert C, Bassi R, Rochaix J-D (2009) Analysis of the chloroplast protein kinase Stt7 during state transitions. PLoS Biol **7:** e45

Li Z, Peers G, Dent RM, Bai Y, Yang SY, Apel W, Leonelli L, Niyogi KK (2016a) Evolution of an atypical de-epoxidase for photoprotection in the green lineage. Nat Plants **2:** 16140

Li X, Zhang R, Patena W, Gang SS, Blum SR, Ivanova N, Yue R, Robertson JM, Lefebvre PA, Fitz-Gibbon ST, et al (2016b) An indexed, mapped mutant library enables reverse genetics studies of biological processes in *Chlamydomonas reinhardtii*. Plant Cell **28:** 367–387

Marschall M, Proctor MCF (2004) Are bryophytes shade plants? Photosynthetic light responses and proportions of chlorophyll *a*, chlorophyll *b* and total carotenoids. Ann Bot **94:** 593–603

Müller-Moulé P, Conklin PL, Niyogi KK (2002) Ascorbate deficiency can limit violaxanthin de-epoxidase activity in vivo. Plant Physiol **128:** 970–977

Müller-Moulé P, Havaux M, Niyogi KK (2003) Zeaxanthin deficiency enhances the high light sensitivity of an ascorbate-deficient mutant of Arabidopsis. Plant Physiol **133:** 748–760

Nagy V, Vidal-Meireles A, Podmaniczki A, Szentmihályi K, Rákhely G, Zsigmond L, Kovács L, Tóth SZ (2018) The mechanism of photosystem-II inactivation during sulphur deprivation-induced H_2 production in *Chlamydomonas reinhardtii*. Plant J **94:** 548–561

Neupert J, Karcher D, Bock R (2009) Generation of *Chlamydomonas* strains that efficiently express nuclear transgenes. Plant J **57:** 1140–1150

Niyogi KK, Bjorkman O, Grossman AR (1997) *Chlamydomonas* xanthophyll cycle mutants identified by video imaging of chlorophyll fluorescence quenching. Plant Cell **9:** 1369–1380

Peers G, Truong TB, Ostendorf E, Busch A, Elrad D, Grossman AR, Hippler M, Niyogi KK (2009) An ancient light-harvesting protein is critical for the regulation of algal photosynthesis. Nature **462:** 518–521

Pinnola A, Dall'Osto L, Gerotto C, Morosinotto T, Bassi R, Alboresi A (2013) Zeaxanthin binds to light-harvesting complex stress-related protein to enhance nonphotochemical quenching in *Physcomitrella patens*. Plant Cell **25:** 3519–3534

Polukhina I, Fristedt R, Dinc E, Cardol P, Croce R (2016) Carbon supply and photoacclimation cross talk in the green alga *Chlamydomonas reinhardtii*. Plant Physiol **172:** 1494–1505

Porra RJ, Thompson WA, Kriedeman PE (1989) Determination of accurate extinction coefficients and simultaneous equations for assaying chlorophylls *a* and *b* with four different solvents: Verification of the concentration of chlorophyll standards by atomic absorption spectroscopy. Biochim Biophys Acta **975:** 384–394

Quaas T, Berteotti S, Ballottari M, Flieger K, Bassi R, Wilhelm C, Goss R (2015) Non-photochemical quenching and xanthophyll cycle activities in six green algal species suggest mechanistic differences in the process of excess energy dissipation. J Plant Physiol **172:** 92–103

Roach T, Na CS (2017) LHCSR3 affects de-coupling and re-coupling of LHCII to PSII during state transitions in *Chlamydomonas reinhardtii*. Sci Rep **7:** 43145

Ruban AV, Johnson MP, Duffy CD (2012) The photoprotective molecular switch in the photosystem II antenna. Biochim Biophys Acta **1817:** 167–181

Saga G, Giorgetti A, Fufezan C, Giacometti GM, Bassi R, Morosinotto T (2010) Mutation analysis of violaxanthin de-epoxidase identifies substrate-binding sites and residues involved in catalysis. J Biol Chem **285:** 23763–23770

Schroda M, Vallon O, Whitelegge JP, Beck CF, Wollman FA (2001) The chloroplastic GrpE homolog of *Chlamydomonas*: Two isoforms generated by differential splicing. Plant Cell **13:** 2823–2839

Smirnoff N (2018) Ascorbic acid metabolism and functions: A comparison of plants and mammals. Free Radic Biol Med **122:** 116–129

Takizawa K, Kanazawa A, Kramer DM (2008) Depletion of stromal P_i induces high "energy-dependent" antenna exciton quenching (q_E) by

decreasing proton conductivity at CF_O-CF_1 ATP synthase. Plant Cell Environ **31:** 235–243

Tikkanen M, Mekala NR, Aro E-M (2014) Photosystem II photoinhibition-repair cycle protects photosystem I from irreversible damage. Biochim Biophys Acta **1837:** 210–215

Tóth SZ, Lőrincz T, Szarka A (2018) Concentration does matter: The beneficial and potentially harmful effects of ascorbate in humans and plants. Antioxid Redox Signal **29:** 1516–1533

Tóth SZ, Nagy V, Puthur JT, Kovács L, Garab G (2011) The physiological role of ascorbate as photosystem II electron donor: Protection against photoinactivation in heat-stressed leaves. Plant Physiol **156:** 382–392

Tóth SZ, Puthur JT, Nagy V, Garab G (2009) Experimental evidence for ascorbate-dependent electron transport in leaves with inactive oxygen-evolving complexes. Plant Physiol **149:** 1568–1578

Ünlü C, Drop B, Croce R, van Amerongen H (2014) State transitions in *Chlamydomonas reinhardtii* strongly modulate the functional size of photosystem II but not of photosystem I. Proc Natl Acad Sci USA **111:** 3460–3465

Urzica EI, Adler LN, Page MD, Linster CL, Arbing MA, Casero D, Pellegrini M, Merchant SS, Clarke SG (2012) Impact of oxidative stress on ascorbate biosynthesis in *Chlamydomonas* via regulation of the *VTC2* gene encoding a GDP-L-galactose phosphorylase. J Biol Chem **287:** 14234–14245

Vidal-Meireles A, Neupert J, Zsigmond L, Rosado-Souza L, Kovács L, Nagy V, Galambos A, Fernie AR, Bock R, Tóth SZ (2017) Regulation of ascorbate biosynthesis in green algae has evolved to enable rapid stress-induced response via the *VTC2* gene encoding GDP-l-galactose phosphorylase. New Phytol **214:** 668–681

Voigt J, Münzner P (1994) Blue light-induced lethality of a cell wall-deficient mutant of the unicellular green alga *Chlamydomonas reinhardtii*. Plant Cell Physiol **35:** 99–106

Wang Z, Xiao Y, Chen W, Tang K, Zhang L (2010) Increased vitamin C content accompanied by an enhanced recycling pathway confers oxidative stress tolerance in *Arabidopsis*. J Integr Plant Biol **52:** 400–409

Wheeler G, Ishikawa T, Pornsaksit V, Smirnoff N (2015) Evolution of alternative biosynthetic pathways for vitamin C following plastid acquisition in photosynthetic eukaryotes. eLife **4:** e06369

Xue H, Tokutsu R, Bergner SV, Scholz M, Minagawa J, Hippler M (2015) PHOTOSYSTEM II SUBUNIT R is required for efficient binding of LIGHT-HARVESTING COMPLEX STRESS-RELATED PROTEIN3 to photosystem II-light-harvesting supercomplexes in *Chlamydomonas reinhardtii*. Plant Physiol **167:** 1566–1578

Zechmann B, Stumpe M, Mauch F (2011) Immunocytochemical determination of the subcellular distribution of ascorbate in plants. Planta **233:** 1–12